Experimental Investigation on Post-tensioned Spannglass Beams during Temperature Loads

M. Engelmann, P. Bukieda & B. Weller

Technische Universität Dresden, Institute of Building Construction, Germany, michael.engelmann@tu-dresden.de

Recent research work focused on material efficient and safe structural use of glass beams. Reinforcing and post-tensioning of those structures in the style of reinforced concrete are promising options. They allow for a safe post-breakage behaviour of load bearing glass constructions. Other ductile materials such as steel and high-grade cables strengthen the glass, which results in robust structures. However, hybrid structures are prone to temperature loads. Especially post-tensioned glass beams – Spannglass Beams – are vulnerable to lose part of their initial cable load caused by a different expansion of their parts. The thermal expansion coefficient of steel cables is about 70% larger than the value of glass. Therefore, a cable in a hybrid structure will expand much more during heating. This effect results in a loss in initial cable load of a post-tensioned reinforcement, and cannot be prevented. Hence, the temperature dependency needs to be considered during the design stage. Furthermore, a change in temperature influences the material properties of glass-contact materials and the interlayer. Thermoplastic blockings transfer the cable load into the laminated glass edge. Due to manufacturing tolerances, the interlayer material is stressed. Therefore, this will affect the reaction of the structure to a change in temperature. The non-destructive experimental study includes the results of a set of two Spannglass Beams with 8 mm post-tensioned cables. Adhesively bonded connectors redirect the cables according to the needs in a four-point bending set-up. Two-meter long beams were placed in a climate chamber to heat the specimens from ambient temperature to 60°C. We recorded the structural behaviour at alternating initial cable loads as well as different bending loads. Finally, the results led to a recommendation on how to consider a possible loss in cable load caused by a change in temperature. This will support the argumentation that post-tensioning glass beams is a feasible structural option.

Keywords: glass beam, post-tensioning, reinforcement, temperature load, temperature compensation, spannglass

1. Introduction

As the use of structural glass increases, the demand for their material efficient use increases as well. This development involves research on hybrid or reinforced load-bearing solutions. Based on concrete design, glass beams are improved by adding ductile materials such as steel into the cross section. At the event of brittle glass failure, the ductile material is still able to carry tensile loads, while the broken glass section bears the compressive component. This results in an increased post-breakage moment capacity of the reinforced glass beam (among others in (Weller et.al. 2010) and (Louter 2011)). Furthermore, post-tension techniques are applied on several structural glass beams. This way a pre-stress is applied to the glass edge that needs to be decompressed first resulting in an increased load capacity while the post-breakage capability provided by the ductile reinforcement remains (Schober et.al. 2004); (Bos et.al. 2004); (Louter et.al. 2006); (Louter et.al. 2012); (Louter et.al. 2013); (Louter et.al. 2014); (Jordão et.al. 2014); (Weller and Engelmann 2014); (Cupac et.al. 2015); (Weller and Engelmann 2015); (Engelmann 2015); and (Firmo et.al. 2015).

Fig. 1 Spannglass-Beam Mock-ups. A large-scale 9,0 m pedestrian bridge at glasstec 2014 in Düsseldorf, Germany.

However, this requires additional detailing and calculation. An internal equilibrium of forces between the glass, the post-tensioned tendon as well as structural glass contact materials and thermoplastic interlayer materials exists.

The effect of a change in temperature on materials is twofold. In an unconstrained situation, every homogeneous material deforms according to its thermal expansion coefficient without building up stresses (Fig. 2, left). In a situation where the strain is hampered, a thermal load leads to thermal stress (Fig. 2, right). Different materials in hybrid structures are supposed to work together structurally, which requires a fixed connection. This results in a partial strain restriction (Fig. 2, centre). In this research steel and glass are connected. The compatibility constraint is met while the total strain of the steel cable equals the strain of the glass construction. Steel expands to a larger degree compared with glass. This difference in strain equals the change in stress in both partners. Heating of a Spannglass-Beam will result in a loss of cable force, which results in a loss of pre-stress.
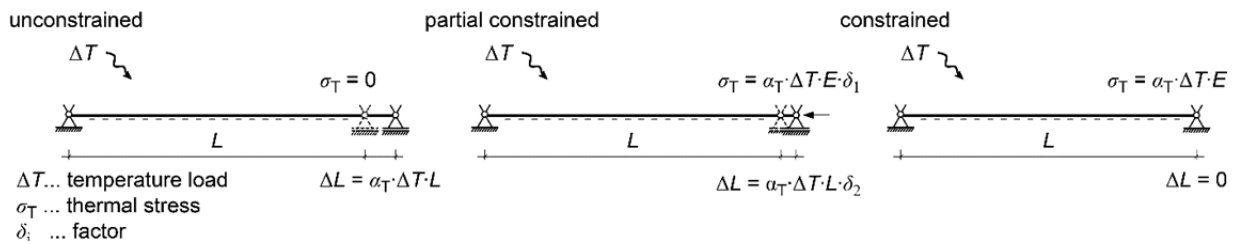
Fig. 2 Thermal stress and strain in constrained and unconstrained beams. A partial constrained may be realized by a cable.

This effect may be addressed analytically by applying linear beam theory. However, in reality we do not meet those assumptions perfectly: imperfections and loading of the interlayer material, which results in a three-dimensional deflection, is omitted. This behaviour is crucial as it initiates stability problems, which leads to early failure. Additionally, interlayer materials such as PVB (among others in Schuler 2003) and structural blocking materials such as POM (Ebert 2014) change their stiffness properties in a relevant temperature range from -20°C to +80°C significantly.

We suspect a significant impact of disregarded effects on the structural reaction. Therefore, we are looking for an experimental description of the temperature effect on Spannglass-Beams by heating specimens in a four-point testing situation up to 60°C. Finally, we compare the analytic and experimental results.as a basis for preliminary design.

This paper is based on previous research in (Weller and Engelmann 2014 and 2015) on Spannglass-Beams during post-tensioning (P) and bending (P+F) by focusing on the additional effects caused by thermal loads (P+F+T).

2. Experimental Methods

2.1. Specimen

Fig. 3 provides the cross section of the Spannglass-Beams. We tested two beams of 2,0 m span, 150 mm height and 52 mm width. Two packages of heat strengthened laminated glass ($\alpha_{T,glass} = 9 \cdot 10^{-6}$ K^{-1} [EN 572-1]), each 2 x 6 mm wide are situated at a gap of 28 mm apart from each other. The gap provided space for a 8 mm spiral cable (PFEIFER PG 5 $\alpha_{T,cable} = 16 \cdot 10^{-6}$ K^{-1} [ETA 11/0160]) with threaded fittings at each end. Stainless steel connectors at the third points of the span connected the packages adhesively and redirected the cable to counteract the external bending load directly (Fig. 3). A stainless steel shoe fixed the glass in a bearing that held the tension nut of the cable (Fig. 4 bottom right). By tightening the nut, the cable was tensioned. The counteracting compressive force was introduced into the laminated glass edge via POM-blockings as described in Weller & Engelmann 2014.
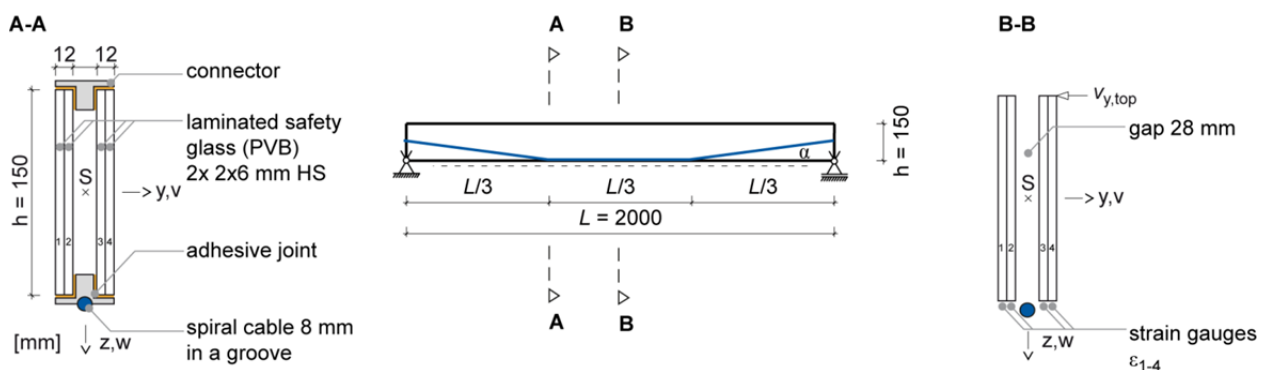
Fig. 3 Specimen sizes and cross section.

2.2. Test Set-up

We were looking for a description of the load bearing behaviour of the beam during thermal and mechanical loads. Therefore, we loaded the specimen in a four-point bending set-up (Fig. 4). A cantilever arm was loaded with concrete blocks and introduced the constant bending load into to the upper glass edge via a loading beam. Before bending, the cables were post-tensioned. We checked the cable load using 10 kN load cells at each cable. Furthermore, we observed the vertical and lateral deflection as well as the strain of the pre-stressed bottom glass edges (Fig. 5, left).
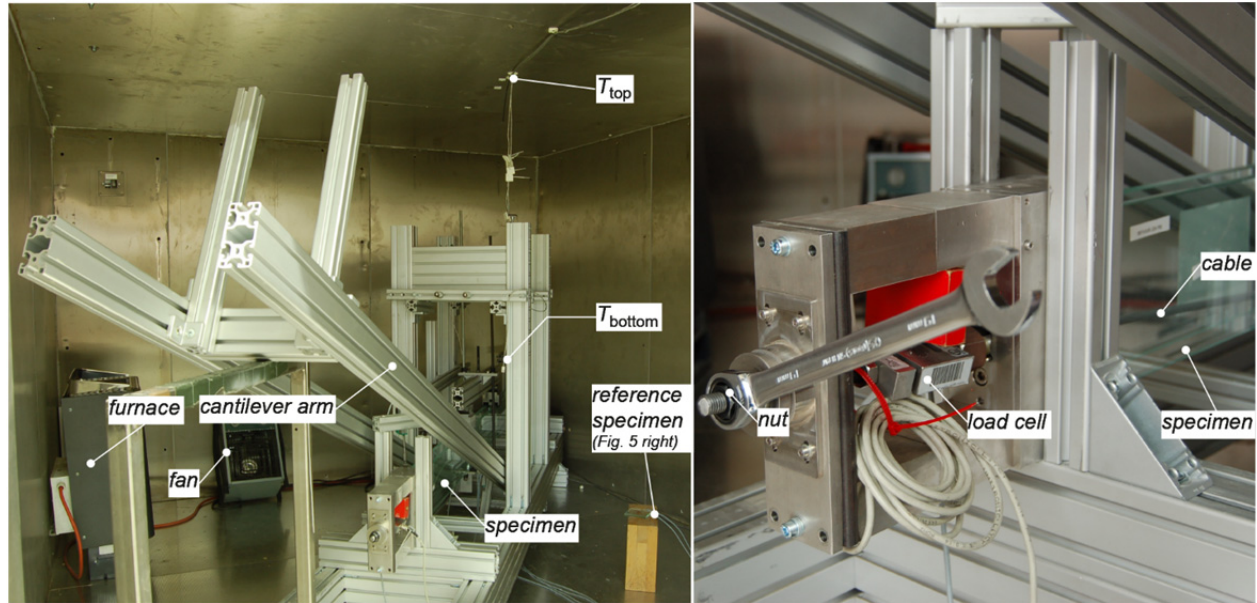
Fig. 4 Test set-up. Climate chamber with furnace and temperature sensors (left). Bearing detail (right).

The set-up was put into a climate chamber where a furnace heated up the ambient air. A fan mixed the air to ensure a constant temperature distribution within the chamber. Two temperature sensors, one below the ceiling (T_{top}) and another one near the glass (T_{bottom}), observed the air temperature (Fig. 5 left). In preliminary tests, we checked the surface temperature of the glass during the heating phase. After four hours (240 min) of heating, the recorded signals near the specimen and the surface temperature reached a constant threshold value of 60 °C and defined the maximum heating time. We give mean values for evaluation between 100 min and 240 min to cover the permanent alteration of the ambient air temperature.
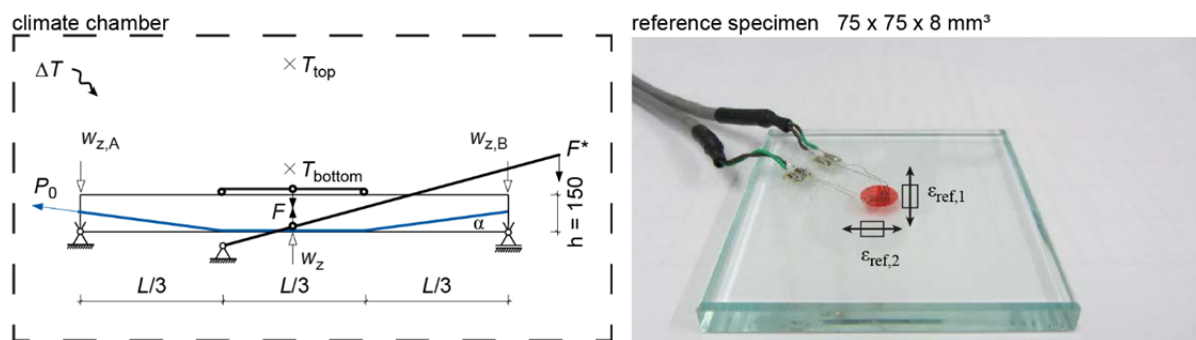
Fig. 5 Arrangement of test set-up (left). Unconstrained reference specimen (right).

2.3. Test Concept and Test Process

We conducted 30 non-destructive four-point bending tests with alternating cable loads and bending loads according to Table 1. The effect of temperature on the un-reinforced glass beam defined reference 1. Furthermore, reinforced beams without cable load showed the effect of reinforcement (reference 2). Finally, an increase in cable load in three steps (3 kN; 6 kN and 9 kN) allowed for a split determination of the following effects on the specimens during heating:

a) Effect of reinforcement by comparing reference 1 with reference 2
b) Effect of post-tensioning by comparing un-reinforced reference 1 with the post-tensioned options
c) Effect of post-tensioning by comparing reinforced reference 2 with the post-tensioned options

The load cases were applied stepwise. First, we stressed the cables and added the bending load during room-temperature. Afterwards, we heated the room to 60°C for four hours and recorded the change in cable load, deflection and deformation. Finally, we unloaded the system by shutting the furnace down for four hours and removed the mechanical loads. The beams were left to settle for the next test.

Table 1 Labelling of tests – 15 non-destructive bending tests for two specimens labelled (I) and (II).

Types of tests		Initial cable load P_0	Bending load F		
			0 kN	5,0 kN	10,7 kN
Reference 1	un-reinforced beams	Without cable	PX_F00	PX_F05	PX_F10
Reference 2	reinforced beams	< 0,1 kN	P0_F00	P0_F05	P0_F10
Objects of investigation	post-tensioned beams	3 kN	P3_F00	P3_F05	P3_F10
		6 kN	P6_F00	P6_F05	P6_F10
		9 kN	P9_F00	P9_F05	P9_F10

2.4. Effect of Temperature on Measuring Devices

A change in temperature affects the measured signal (Keil 1995). Load cells use an internal compensation of temperature (Wheatstone bridge) while inductive displacement gauges are not prone to a change in temperature by manufactures data. All used devices were placed in an oven during a preliminary study where they were able to expand unconstrained during the heating-phase up to 80°C, which is 33% higher than the aspired temperature load of the beams. The tests confirmed that the displacement gauges and the load cells do not suffer from a change in ambient temperature. Strain gauges showed a significant reaction when prone to a change in temperature. Therefore, we give a method for temperature compensation (Keil 1995; Vishay 2010).

2.5. Temperature Compensation

The total strain from the measured signal contains parts of mechanical strain due to bending and parts from thermal strain. A strain gauge cannot determine the reason for a change in deformation. Linear beam theory gave the mechanical strain ε_{mech} (Weller & Engelmann 2014). It was checked during the reference tests (PX_F05; PX_F10; P3_F00; P6_F00 and P9_F00). The mechanical strain caused by each bending load F was constant during the tests. The cable load P was recorded during the test. So, its effect on the strain of the glass edge was calculated using those results. This covers the effect of F on P in the statically undetermined system. The thermal strain ε_{therm} remained unknown, but was calculated by removing the mechanical part from the total signal, Equation (1).

$$\varepsilon_{signal} = \varepsilon_{mech} + \varepsilon_{therm} = \varepsilon_F + \varepsilon_P + \varepsilon_{therm}$$

where

$$\varepsilon_F = \frac{F \cdot L}{4 \cdot t \cdot h^2 \cdot E_{glass}}$$

$$\varepsilon_P = -\frac{P \cdot \sin(\alpha) \cdot L}{4 \cdot t \cdot h^2 \cdot E_{glass}}$$

ε_{signal} ...*recorded strain signal*
ε_{mech} ...*mechanical strain*
ε_F ...*bending strain caused by bending load F*
ε_P ...*bending strain caused by cable force P*
ε_{therm} ...*thermal strain*
t ...*glass thickness* (6 mm)
h ...*glass height* (150 mm)
E ...*glass Youngs Modulus* (70.000 N / mm²)

(1)

We used single strain gauges (quarter bridges) to measure the strain at the glass edge ε_{signal}. The effect of temperature on the gauge is threefold:

a) Thermal strain of the grid.
b) Thermal strain of the gauges foil.
c) Temperature dependencies of the connection wires (found to be not significant).

A Wheatstone bridge that contains four electrical resistances compensates those effects. During this study, the strain of four glass edges per specimen were recorded, which required an uneconomical large number of gauges. Therefore, we used quarter bridges and removed the effect of a change in temperature ΔT by calculation.

The application of a strain gauge on an object fixes their relative strain and leads to constraints (Fig. 6). The thermal expansion of the gauge differs from the thermal expansion of the material. Thus, during heating the gauge cannot deform freely, which leads to a signal depending on the difference in expansion of the object and the gauge (ε_{app}).

This difference is given by the manufacturer in relation to a defined material. So the thermal expansion of the gauge equals the thermal expansion coefficient of the applied material (α_{gauge}= 11,8 · 10^{-6} K^{-1}). Doing so leads to the full removal of the recorded signal during a change in temperature. The thermal strain will not be recorded.
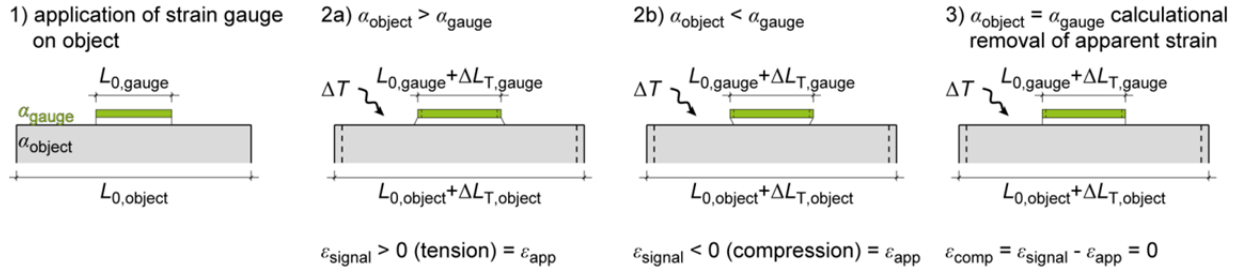
Fig. 6 Removal of apparent strain. The scheme illustrates the difference in unconstrained strain. This difference causes a measured signal. In reality, we assume the same strain of the gauge and the object.

The manufacturer gave a polynomial to describe the apparent strain, Equation 2. Its reference is 20°C ($T_{20} = \Delta T + 20$ K). We chose gauges with considerably small apparent strain. Fig. 8 depicts the apparent strain near zero during the tests.

$$\varepsilon_{app}(T) = -3,60 \cdot 10^1 + 2,65 \cdot 10^1 \cdot T_{20}^1 - 4,63 \cdot 10^{-2} \cdot T_{20}^2 + 1,88 \cdot 10^{-4} \cdot T_{20}^3 - 2,61 \cdot 10^{-18} \cdot T_{20}^4 \left[\frac{\mu m}{m} \right] \tag{2}$$

The given relation referred to a k-factor of 2,0. So, an adaption to the k-factor of each individual gauge (k* = 2,1) was necessary, Equation 3. Additionally, the k-factor changes with temperature. The used gauges in this study do not suffer significantly from this effect in the prospected temperature range. Thus, it was not necessary to cover this effect.

As we wished to include the thermal strain of the object (Fig. 7), we had to remove the thermal strain of the strain gauge by calculation as well. This left the signal with all elements according to Equation (1) and resulted in the compensated strain ε_{comp} according to Equation (3).

$$\varepsilon_{comp}(T) = \varepsilon_{signal} - \varepsilon_{app} \cdot \frac{k}{k*} - \alpha_{gauge} \cdot \Delta T \quad where \quad \frac{k}{k*} = \frac{2,0}{2,1} \tag{3}$$
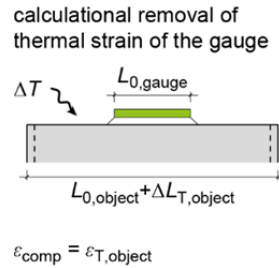
Fig. 7 Removal of the strain of the gauge results in the thermal strain of the object.

3. Results

3.1. Unreinforced Reference

The test set-up included a reference specimen (Fig. 5 right) to record the unconstrained strain of the glass. Its signal was compensated according to Equation (3), too. Fig. 8 depicts the signal of the unloaded reference beam P0_F0 (ε_{signal}) as well as the signal of the reference specimen (ε_{ref_signal}) during heating. Even so, the strain was unrestricted, the signal was negative indicating compressive strain during heating. This illustrates situation 2b) in Fig. 6 and was compensated. The results after compensation (ε_{comp} and ε_{comp_ref}) are printed versus the unconstrained strain of glass, Equation (4).

$$\varepsilon_{T,glass}(T) = \alpha_{T,glass} \cdot \Delta T \quad where \quad \alpha_{T,glass} = 9,0 \cdot 10^{-6} \cdot K^{-1} \tag{4}$$

The maximal deviation between the unloaded beam and the reference specimen was 28,34 μm/m at an average of 15,66 μm/m between 100 min and 240 min of heating. It means that the reference specimen is usable to record the unconstrained thermal strain of the glass beam. Those results were used as an indication for the error margin. The unconstrained strain according to Equation (4) was bordered by the compensated strain of the reference specimen and the unloaded beam. Thus, the compensation procedure was usable to calculate the occurring thermal strain. Furthermore, the values varied according to the change in ambient temperature in the chamber. We used the mean temperature during this time range for further evaluation (mean $\Delta T = 62,6$ °C in Fig. 8).
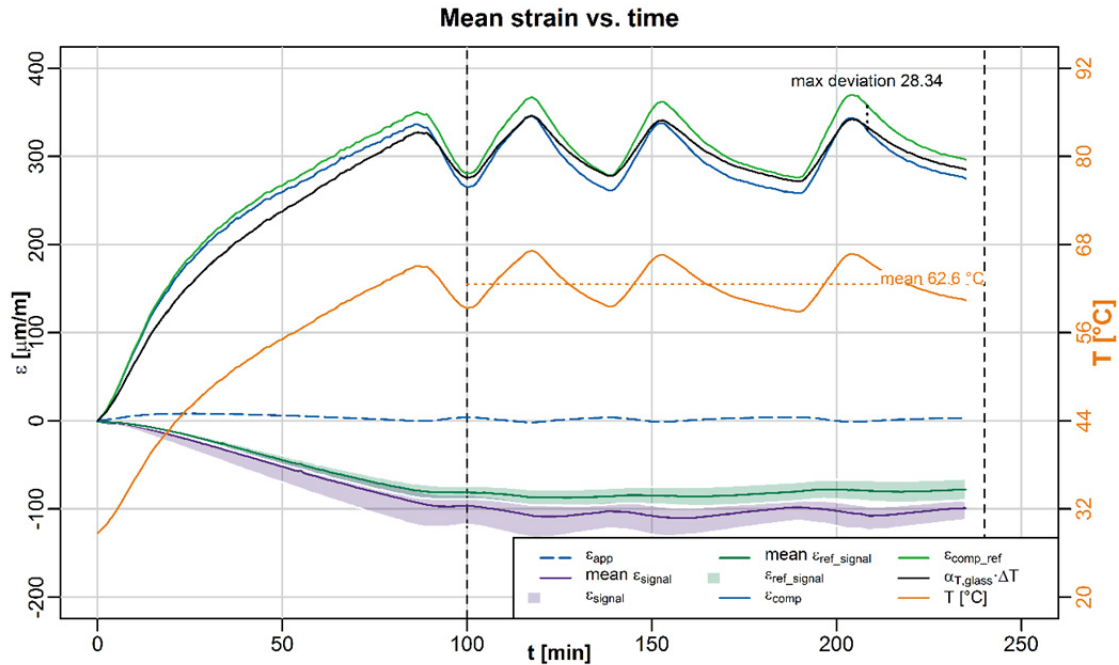
Fig. 8 Signals of unloaded specimen during heating, compensated signals and strain of the glass according to Equation (4). The apparent strain shows to be near zero.

3.2. Reinforced Reference ($P_0 = 0$)

Table 2 gives the results for the blank un-reinforced and the reinforced beams as a reference. The mean thermal coefficient of the whole beam (Equation (5)) for all bending loads showed to be $9,07 \pm 0,51$ μm/mK. The standard deviation spread from the acquired 9,0 μm/mK. Therefore, we conducted further analysis in groups to respect the loading situation of each specimen.

$$\alpha_{T,beam} = \frac{\Delta\varepsilon_{comp}}{\Delta T} \tag{5}$$

$$\Delta\varepsilon_{comp} = mean\ \varepsilon_{comp}\left(t = 100\ to\ 240\ \text{min}\right) - \varepsilon_{comp}\left(t = 0\right) \tag{6}$$

Table 2: Change in strain versus change in ambient temperature. $\Delta T = 36,6 \pm 2,5$ K (mean ± standard deviation).

Specimen	ΔT [K]		$\Delta\varepsilon_{comp}$ [μm/m]		$\Delta\varepsilon_{comp} / \Delta T$ [μm/mK]	
	spec (I)	spec (II)	spec (I)	spec (II)	spec (I)	spec (II)
PX_F00	33,9	33,5	295,9	274,2	8,72	8,17
PX_F05	38,4	40,9	356,5	376,0	9,28	9,20
PX_F10	40,1	38,3	378,4	368,0	9,43	9,61
mean ± standard deviation (PX)					$9,07 \pm 0,53$	
P0_F00	36,3	37,6	318,2	313,7	8,77	8,35
P0_F05	35,2	37,0	320,4	328,1	9,09	8,87
P0_F10	34,9	33,4	342,6	319,1	9,81	9,55
mean ± standard deviation (P0)					$9,07 \pm 0,53$	
mean ± standard deviation (P0 and PX)					$9,07 \pm 0,51$	

3.3. Post-tensioned Beams

It took 100 minutes to heat the chamber. Afterwards the ambient air temperature ranged according to the control system of the furnace. The graph Fig. 9 shows the change in temperature for specimen (I) P6_F0 only. The value at the bottom, near the specimen (T_{bottom}), varied between 58.8 °C and 67,2 °C with a mean value of 62,6 °C. Below the ceiling of the chamber, about 1 m above the specimen, the mean ambient temperature was 5,2 K higher (Fig. 9).

During heating specimen (I) showed a drop in cable load to 85 % from 5,96 kN to 5,09 kN (dark blue line in Fig. 9). After 4 hours the cable load remains almost unchanged at 5,10 kN. This corresponded to a change in cable load by 0,87 kN / 35,4 K = 24,6 N/K. In contrast, Table 3 gives the mean values between 100 min and 240 min of heating. After heating the cable load varied according to the ambient temperature with smallest cables loads at temperature peaks and highest cable loads during low temperatures. There was no considerable shift between maximus and minimums of temperature and cable load. The system reacted actively, thus the chosen temperature scenario as well as the analysis of mean cable load is reasonable.

The results of specimen (I) and specimen (II) in Fig. 9 overlap or run parallel. Thus, the experiments were well replicable. As each test ran individually, the progression of the air temperature differed. In Fig. 9 the first peak in temperature was recorded before 100 min. This is the main cause for the deviation between two similar specimens. Additionally, there was an initial deviation in cable load. P6_F10 in Fig. 9 starts at 7,39 kN (specimen (I)) and 7,59 kN (specimen (II)). This resulted in a parallel arrangement of the dashed and continuous purple lines rather than an overlap. The detailed results listed in Table 3 showed a decrease in cable load during heating between 78 % and 95 %.
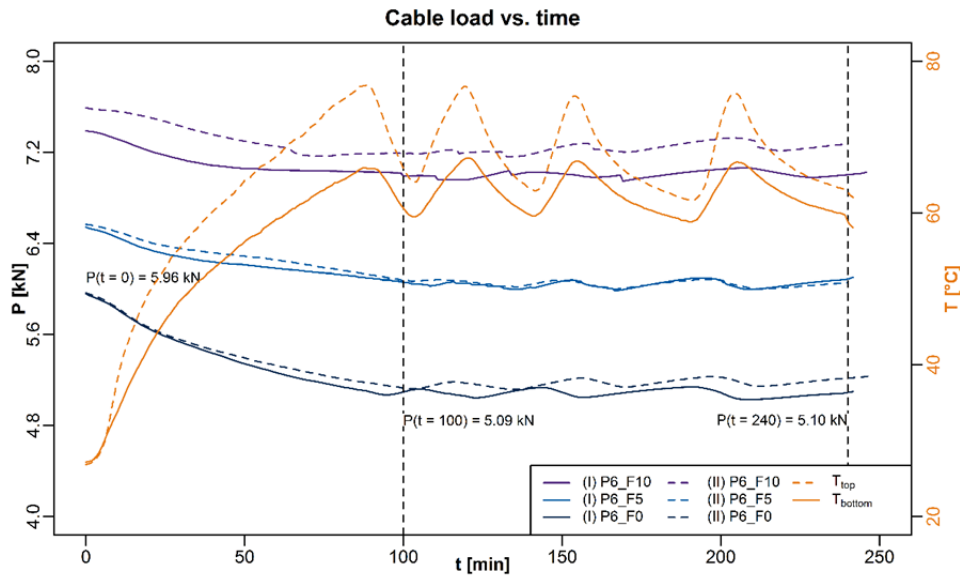
Fig. 9 Change in cable load, specimens (I) and (II) at an initial cable load of $P_0 = 6$ kN. Temperature for specimen (I) P6_F0.

Table 3: Loss in cable load. $\Delta T = 37,4 \pm 2,9$ K (mean ± standard deviation).

Specimen	P(t = 0) [|kN]		mean P(t = 100 to 240 min) [kN]		ΔT [K]	
	specimen (I)	specimen (II)	specimen (I)	specimen (II)	specimen (I)	specimen (II)
P3_F00	3,00 (100%)	3,08 (100%)	2,35 (78%)	2,41 (78%)	36,7	36,3
P3_F05	3,64 (100%)	3,62 (100%)	3,09 (85%)	3,13 (86%)	44,0	39,3
P3_F10	4,48 (100%)	4,46 (100%)	4,15 (93%)	4,22 (95%)	40,3	36,4
P6_F00	5,96 (100%)	5,96 (100%)	5,08 (85%)	5,17 (87%)	35,4	39,7
P6_F05	6,54 (100%)	6,57 (100%)	6,04 (92%)	6,04 (92%)	43,5	39,0
P6_F10	7,39 (100%)	7,59 (100%)	7,00 (95%)	7,24 (95%)	34,7	39,2
P9_F00	8,98 (100%)	9,01 (100%)	7,95 (89%)	7,95 (88%)	36,7	36,7
P9_F05	9,46 (100%)	9,52 (100%)	8,99 (95%)	9,05 (95%)	40,2	36,1
P9_F10	10,39 (100%)	10,52 (100%)	9,87 (95%)	9,89 (94%)	35,1	32,2

As a second example, Fig. 10 shows the analysis of recorded strain at the glass edge during P9_F10 test of specimen (I). The bending load of F = 10,7 kN resulted in a tensile strain of ε_F = 566,1 μm/m. From the cable load we determine a compressive strain of ε_P = -122,9 μm/m at the beginning and ε_P = -116,8 μm/m during the hot phase. The loss in cable load of 0,5 kN resulted in a loss in compression of 6,11 μm/m. This is lower than the error margins in Fig. 8. Thus, the change in compensated strain of 359,9 μm/m ($\Delta\varepsilon_{comp}$; purple line in Fig. 10) resulted from thermal expansion only. It yielded at 113% of the change in unrestrained thermal strain of the reference specimen (318,8 μm/m). We will focus on the change in cable load, as the change in mechanical strain is comparatively low.
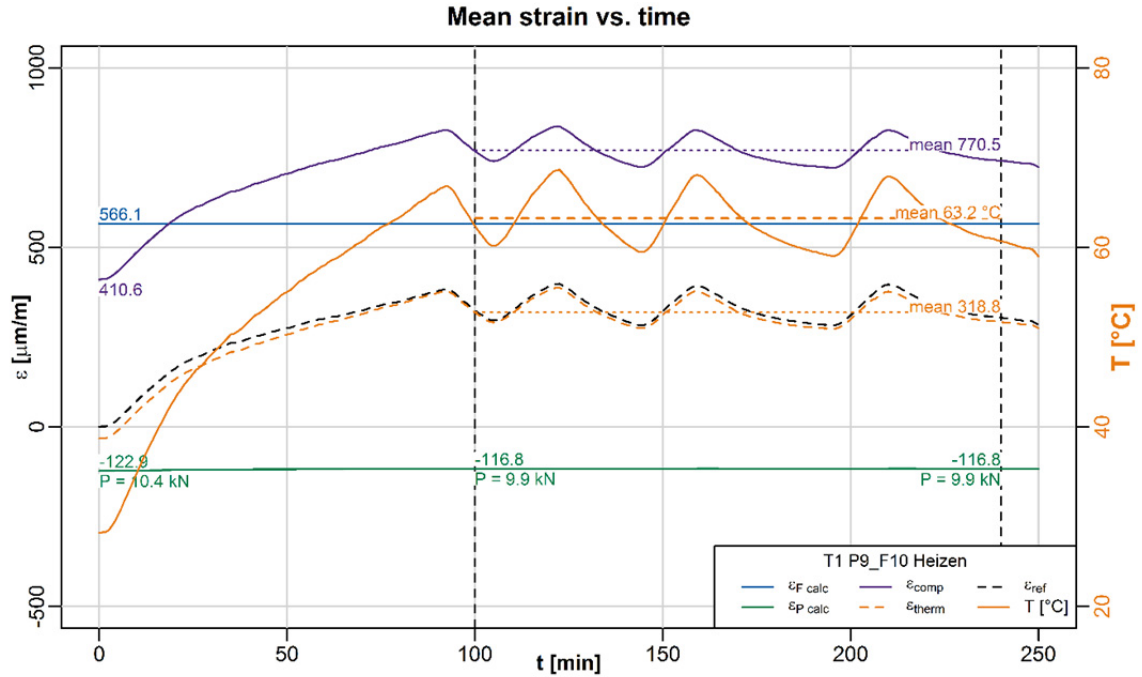
Fig. 10 Thermal and mechanical strain for specimen (I) P9_F10.

Table 4 summarizes the relative change in cable load and the relative change in strain to give a common basis for comparison. As the ambient air temperature changed during the hot phase of the test, we used mean values of cable load, strain and temperature between 100 minutes and 240 minutes. (Equation 6-8)

$$\Delta P = mean\ P(t = 100\ to\ 240\ \text{min}) - P(t = 0) \tag{7}$$

$$\Delta T = mean\ T(t = 100\ to\ 240\ \text{min}) - T(t = 0) \tag{8}$$

Table 4: Loss in cable load and change in strain versus change in ambient temperature.

Specimen	ΔP [kN]		ΔP / ΔT [N/K]		$\Delta\varepsilon_{comp}$ [μm/m]		$\Delta\varepsilon_{comp}$ / ΔT [μm/mK]	
	spec (I)	spec (II)	spec (I)	spec (II)	spec (I)	spec (II)	spec (I)	spec (II)
P3_F00	-0,647	-0,678	-17,6	-18,7	328,5	311,0	8,96	8,57
P3_F05	-0,548	-0,492	-12,5	-12,5	430,7	371,5	9,79	9,46
P3_F10	-0,327	-0,244	-8,1	-6,7	406,8	357,1	10,10	9,82
P6_F00	-0,874	-0,793	-24,7	-20,0	316,4	353,6	8,94	8,91
P6_F05	-0,502	-0,524	-11,5	-13,4	430,8	369,3	9,90	9,46
P6_F10	-0,385	-0,354	-11,1	-9,0	341,9	397,0	9,84	10,12
P9_F00	-1,030	-1,058	-28,1	-28,8	337,6	321,6	9,20	8,77
P9_F05	-0,466	-0,463	-11,6	-12,8	384,0	337,8	9,56	9,36
P9_F10	-0,518	-0,627	-14,8	-19,5	359,8	325,0	10,26	10,08
mean ± standard deviation (P3, P6 and P9)							9,50 ± 0,52	

The cable load of the unloaded beams (F00) dropped on average by -23,0 N/K. After bending (F05 and F10), the cable shared the total bending load with the glass, which resulted in an increase in cable load. However, those options lose between -12,4 N/K and -11,5 N/K on average. The same tendency referred to the drop in mean strain. As the bending load increased, we recorded an increase in change of tensile strain during heating. It yielded at a mean of $9,50 \pm 0,52$ µm/mK.

4. Discussion

4.1. Strain of the glass edge

During the heating of the specimen, the cable as well as the glass and all other components expanded. Table 3 shows the change in temperature, while Table 4 gives the resulting compensated strain. Using their relation leads to the evaluation of the thermal expansion coefficient of the beam $\alpha_{T,beam}$. Fig. 11 shows this value grouped by reinforcement type and bending load. First of all, the change in strain is considerably close to the reference strain of the unconstrained glass specimen of $9,0 \cdot 10^{-6}$ K^{-1}. Those numbers reflect the fact that the loaded cables do not restrict the thermal expansion of the glass significantly. This leads to the conclusion that there is no significant thermal stress present during this study. The glass beams expand almost unhampered. This is caused by the fact that the steel expands to a larger degree ($\alpha_{T,steel} > \alpha_{T,glass}$) leaving space for the glass to expand during heating.

The unreinforced beam (blue in Fig. 11 left) showed an average expansion larger than glass. Compared to the reinforced reference and the post-tensioned specimen there was no significant change in the mean values at a 95% confidence level. The same referred to the comparison of options of different initial cable loads. The plot depicts an increase of maximum and minimum values as the initial cable load increases. We conclude that the initial cable load does not influence the given change significantly.
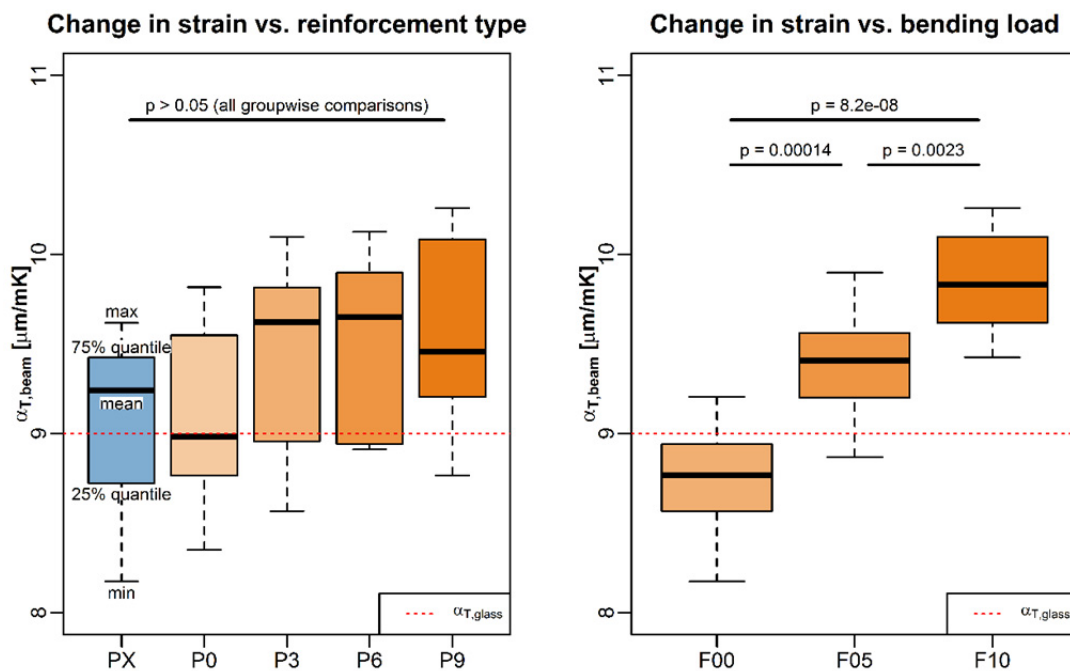
Fig. 11 Change in strain grouped by reinforcement type (left) and bending load (right) including t-test results at 95% confidence level.

Looking at Fig. 11 (right) the level of bending load has a significant effect on the thermal strain of the beam ($p < 0.05$). During heating, the cable load decreased and reduced the initial uplift of the post-tensioned beam. The bending load causes a deflection in the same direction. As the cable escapes from the load sharing between the glass and the reinforcement, the glass needs to carry a larger proportion of the bending load. Thus, the bending load conducts physical work and is a significant variable in the calculation of the change in cable load during heating.

4.2. Cable load P

The cable force dropped during heating of the specimen. Thus, the striven effect of post-tensioning reduced during this stage. The results showed an average drop of -23,0 N/K of the unloaded beams and a loss of -12,4 N/K and -11,5 N/K of the loaded beams. The different systems caused this variance. The unloaded beam (F = 0) is statically determined, as it is only loaded by the cable force, which may be replaced by the forces acting at each connecting point. During bending of the post-tensioned Spannglass-Beams, the cable load increases. The cable load is a function of the bending load in the statically undetermined system.

However, as a result the authors point out that a post-tensioned beam may lose its pre-compressed property during heating. As an example we use P3_F05 from Table 4 with $\Delta P / \Delta T = -12,5$ N/K. Let us assume an installation at +5 °C in a mild winter day and a maximal heating up to 75 °C during the following hot summer. The beam will lose 0,87 kN or 29 % of its initial cable load. This corresponded with an increase in tensile stress in the glass and was considered crucial. Furthermore, the time-depended loss due to creeping and relaxation within the structure is not included yet. So, a glass beam with unbonded tendons needs to have a minimum initial cable load to make sure that during a worst case temperature scenario the cable will still carry a significant part of the total bending load. The given experimental results will be used to verify analytical and numerical models to come up with a tool to design Spannglass-Beams for thermal loads.

We conducted non-destructive tests. After heating, the specimen cooled down to room temperature and showed an acceptable reversal of cable load and strain. The given relations will work for a negative change in temperature during the given boundary conditions as well. Thus, during cooling the cable load increases and may reach the highest values during a negative temperature scenario that will lead to relevant design loads. In an eccentric reinforcement configuration, the post-tensioning will stress the upper glass edge. An increase in cable load leads to an increase in axial load and bending in the glass, which will result in a possible failure in stability.

4.3. Effect of reinforcement

Reinforcing a glass beam is supposed to increase its post-breakage performance: the steel cable will carry tensile loads, which cannot be covered by the broken glass any more. Fig. 11 (left) shows no significant difference between reinforced and plain specimen. Additionally, Table 2 shows the same thermal expansion coefficient of the blank and reinforced reference beams of 9,07 K^{-1}. Thus, their expansion may be taken as equal and unconstrained.

The reinforced beam ($P_0 = 0$) will lose contact to the cable during heating due to the fact that the steel cable expands to a larger degree compared with the glass. So, in a scenario with broken glass and an increased temperature, the cable cannot support unless the deflection after failure cancels the gap between the glass and the cable. This underlines the need for a minimum initial cable load for a durable use of the unbonded reinforcement.

4.4. Effect of post-tensioning

Post-tensioning showed no significant effect during heating (Fig. 11 left). Thus, the amount of initial cable load was no parameter when calculating the change in cable load during thermal loading. The reason is that the initial cable does not achieve physical work when the specimen is heated up. The bending load and a change in ambient temperature conducts work on the Spannglass-Beam only (Fig. 11 right). These findings need to be underlined by analytic beam theory as well as a numerical study that covers additional effects from uneven load transfer into the laminated glass edge and nonlinear lateral deflection.

5. Conclusion and Summary

In summary, post-tensioning techniques on glass beams show to be a promising option. It increases the load-bearing capacity and the post-breakage performance. Hence, it is an important safety feature. Additionally, it grants the possibility to uplift the structure as needed and accommodate dead load deflection for instance. However, a loss in compressive pre-stress is suspected during a change in temperature.

Therefore, we conducted non-destructive bending tests with two similar specimens at a variety of initial cable loads and bending load. The change in cable load, deflection and deformation was recorded during heating of the beams. A change in temperature influences the measured signal of the strain decisively, which makes an experimental evaluation challenging. Therefore, we gave a method for the compensation of this effect. Using those results, the paper describes the behavior of Spannglass-Beam, especially the effect of heating on the cable load, during a temperature load.

Un-reinforced specimen showed an unconstrained deformation which resulted in a thermal expansion coefficient of the whole beam close to the unconstrained deformation of blank glass.

After reinforcing ($P_0 = 0$), we recorded the same result. The reason was the opening of a gap between the cable and the glass due to different thermal expansion of both materials. The effect of reinforcing is lost. Therefore, a minimum initial cable load is necessary to ensure a mutual load transfer during the planned temperature range. On the contrary, a cooling of those beams leads to an increase in cable load, which may become relevant for the ultimate design of the cable and the stability of the glass.

The results of the post-tensioned options showed a slight increase in thermal expansion coefficient. However, this was found to be non-significant. The initial cable load is no parameter for the calculation of the change in cable load during a change in temperature.

This study was limited to two specimen of the same geometry. We have to look at a broader set of glass sizes and reinforcement layout to be able to calculate the thermal load bearing behaviour of Spannglass-Beams.

Altogether, the results showed that the decrease in cable load is present during heating, but does not lead to a full loss. The given recommendations will help to support the understanding of Spannglass-Beams for safer and transparent structural solution.

Acknowledgements

References

Bos, F. P.; Veer, F. A.; Hobbelmann, G. J.; Louter, P.C.: Stainless Steel Reinforced and Post-Tensioned Glass Beams. In: Proceedings of ICEM12 - 12th International Conference on Experimental Mechanics, 2004.

Bukieda, P.: Spannglass Beams under Temperature Load. Diploma Thesis, Technische Universität Dresden, 2016. (unpublished)

Cupac, J.; Louter, C.:Post-tensioned Structural Glass Beams – Comparative Experimental Study. In: Advanced Building Skins 2015 Conference Proceedings. Published by Englhardt, O. Graz, 2015, pp. 166-172. (draft publication)

Ebert, J.: Einleitung hoher Lasten in Glaskanten – Ein Beitrag zum Einsatz von Kunststoffen als Klotzungsmaterial. Dissertation. Technische Universität Dresden, 2014.

Engelmann, M.: Spannglass-Bridge. Footbridge-design competition contribution. Young Engineers Workshop at IABSE Conference Nara, 2015. doi: 10.13140/RG.2.1.4379.2480

EN 572: Glass in building – Basic soda lime silicate glass products. Part 1: Definitions and general physical and mechanical properties. Berlin, Beuth 2012.

European Technical Approval 11/0160: PFEIFER Wire Ropes. 2011.

Firmo, F.; Jordão, S.; Neves, L.-C.; Ferreira, C.-A.; Goncalves, A.-C.: Structural Behaviour of Simple and Pre-stressed Hybrid Steel-Glass Beams. In: Proceedings of RehabStructures 2015. Azores, Portugal.

Jordão, S.; Pinho, M.; Martins, J.P.; Santiago, A.; Cruz, P.J.S.: Numerical modelling of a laminated beam reinforced with pre-stressed cables. Proceedings of Challenging Glass 4 & COST Action TU0905 Final Conference 2014. Lausanne, Switzerland, pp. 253-260.

Jordão, S.; Pinho, M.; Martins, J. P.; Santiago, A.; Neves, L. C.: Behaviour of laminated glass beams reinforced with pre-stressed cables. Steel Construction, 7 (2014), pp. 204-207. doi: 10.1002/stco.201410027

Keil, S.: Beanspruchungsermittlung mit Dehungsmessstreifen. Zwingenberg, CENEUS, 1995.

Louter, P.C.; van Heusden, J.F.; Veer, F.A.; Vambersky, J.N.J.A.; de Boer, H.R.; Versteegen, J.: Post-tensioned Glass Beams. Proceedings of ECF. 2006.

Louter, C.: Fragile yet Ductile. Structural Aspects of Reinforced Glass Beams. Dissertation TU Delft, 2011.

Louter, C.; Belis, J.; Veer, F.; Lebet, J.-P.: Structural response of SG-laminated reinforced glass beams; experimental investigations on the effects of glass type, reinforcement percentage and beam size. Engineering Structures, 36, 292-301 (2012). doi:10.1016/j.engstruct.2011.12.016

Louter, C.; Pérez, A.; Jordan, T.; Lebet, J.-P.: Post-tensioned structural glass beams – Experimental investigations. In: Proceedings of COST Action TU 905, Mid-term Conference on Structural Glass 2013. Poreč, Croatia, pp. 277-284.

Louter, C.; Cupac, J.; Lebet, J-P.: Exploratory experimental investigations on post-tensioned structural glass beams. In: Journal of Facade Design and Engineering 2 (2014), pp. 3–18. doi: 10.3233/FDE-130012

Schuler, C.: Einfluss des Materialverhaltens von Polyvinylbutyral auf das Tragverhalten von Verbundsicherheitsglas in Abhängigkeit von Temperatur und Belastung. Dissertation. Technische Universität München, 2003.

Schober, H.; Gerber, H.; Schneider, J.: Ein Glashaus für die Therme in Badenweiler. In: Stahlbau 73 (2004). pp. 886-892. doi: 10.1002/stab.200490213

Vishay: Tech Note TN-504-1. Thermisches Ausgangssignal aus DMS und K-Faktor-Änderung mit der Temperatur. 2010.

Weller, B; Meier, A.; Weimar, T.; Menkenhagen, J.; Koschecknick, K.: Hybride Glasträger als Fassadenelemente. In: Stahlbau Spezial – konstruktiver Glasbau 2010, pp. 41-45. Ernst & Sohn (2010). doi: 10.1002/stab.201001306

Weller, B., Engelmann, M.: Deformation of Spannglass Beams Subject to Post-Tensioning. Proceedings of Challenging Glass 4 & COST Action TU0905 Final Conference 2014. Lausanne, Switzerland, pp. 285-294.

Weller, B.; Engelmann, M.: Spannglasträger – Glasträger mit vorgespannter Bewehrung. In: Glasbau 2014. Published by Weller, B.; Tasche, S. Berlin: Ernst & Sohn, 2014, pp. 193-203. doi: 10.1002/stab.201490059

Weller, B., Engelmann, M.: An Innovative Concept for Pre-stressed Glass Beams. In: Proceedings of IABSE Conference. Nara, 2015, pp. 132-133. CD-ROM Full Paper.